ACS OMEGA

Article

Cite This: ACS Omega 2019, 4, 18793−18802

http://pubs.acs.org/journal/acsodf

Photoexcited Toluidine Blue Inhibits Tau Aggregation in Alzheimer's Disease

Tushar Dubey,[†,‡] Nalini Vijay Gorantla,[†,‡] Kagepura Thammaiah Chandrashekara,[§] and Subashchandrabose Chinnathambi*[,†,‡]

[†]Neurobiology Group, Division of Biochemical Sciences, CSIR-National Chemical Laboratory, Dr. Homi Bhabha Road, 411008 Pune, India

[‡]Academy of Scientific and Innovative Research (AcSIR), 411008 Pune, India

[§]Institution of Excellence, Vijnana Bhavan, University of Mysore, Manasagangotri, 570006 Mysore, India

Supporting Information

ABSTRACT: The aggregates of microtubule-associated protein Tau are considered as a major hallmark of Alzheimer's disease. Tau aggregates accumulate intracellularly leading to neuronal toxicity. Numerous approaches have been targeted against Tau protein aggregation, which include application of synthetic and natural compounds. Toluidine blue is a basic dye of phenothiazine family, which on irradiation with a 630 nm light gets converted into a photoexcited form, leading to generation of singlet oxygen species. Methylene blue is the parent compound of toluidine blue, which has been reported to be potent against tauopathy. In the present work, we studied the potency of toluidine blue and photoexcited toluidine blue against Tau aggregation. Biochemical and biophysical analyses using sodium dodecyl sulfate-polyacrylamide gel electrophoresis, ThS fluorescence, circular dichroism spectroscopy, and electron microscopy suggested that toluidine blue inhibited the aggregation of Tau in vitro. The photoexcited toluidine blue potentially dissolved the matured Tau fibrils, which indicated the disaggregation property of toluidine blue. The cell biology studies including the cytotoxicity assay and reactive oxygen species (ROS) production assay suggested toluidine blue to be a biocompatible dye as it reduced ROS levels and cell death. The photoexcited toluidine blue modulates the cytoskeleton network in cells, which was supported by immunofluorescence studies of neuronal cells. The studies in a UAS Tau E14 transgenic *Drosophila* model suggested that photoexcited toluidine blue was potent to restore the survival and memory deficits of *Drosophila*. The overall finding of our studies suggested toluidine blue to be a potent molecule in rescuing the Tau-mediated pathology by inhibiting its aggregation, reducing the cell death, and modulating the tubulin levels and behavioral characteristics of *Drosophila*. Thus, toluidine blue can be addressed as a potent molecule against Alzheimer's disease.

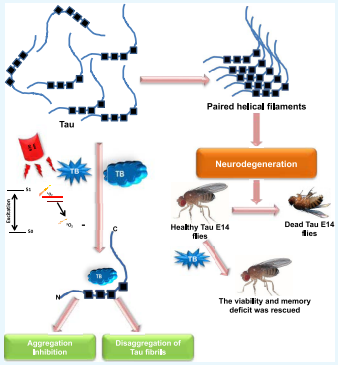

INTRODUCTION

Alzheimer's disease (AD) is a progressive neurodegenerative disorder characterized by decline in the cognitive function, inefficacy to perform regular work, social withdrawal, and poor judgment. AD is associated with short-term memory loss, which predominantly affects CA1, CA3, and dentate gyrus regions of hippocampus. Extracellular senile plaques composed of amyloid-β (Aβ) and intracellular neurofibrillary tangles (NFTs) are the hallmarks of AD.[1−4] In physiological conditions, Tau is found to be associated with microtubules and functions to stabilize the microtubules. In pathological conditions, Tau undergoes various post-translational modifications, oxidative stress, and truncation, resulting in its aggregation.[5−9] The molecules that are potent in inhibiting the aggregation of Tau fibrils are now being considered as a therapeutic for AD.[5,10] Small molecules of natural and synthetic origin were being studied extensively for their medicinal potency against AD pathology.[3,6,7,11] Dyes have been reported for their medicinal potency in AD, and different classes of dyes including porphyrins, phenothiazine, xanthine, etc. showed therapeutic potency in AD. Certain dyes have the property of photoexcitation and are applied in the treatment of several dermatological, microbial, and cancerous disorders. Photodynamic therapy (PDT) or the application of photoexcited (PE) dyes is widely used for the treatment of carcinomas, biofilms, dental plaques, dermatological problems, etc. Photoexcited toluidine blue (TB) is widely used as bactericide, but its effect on neuronal degeneration is yet to be addressed. Principally, the therapy is based on targeting the disaggregation potency of photoexcited dyes against pathological protein aggregates. PDT was found to be effective in inhibiting amyloid-β aggregation and increasing its disaggregation by employing xanthene and porphyrin dyes. TB has been reported for its inhibitory properties against proteins like prion, amyloid-β, Tau, etc.[12−14] Methylene blue (MB) and its derivatives were found to be more potent against AD.[15]

Received: August 29, 2019
Accepted: September 19, 2019
Published: October 29, 2019

DOI: 10.1021/acsomega.9b02792
ACS Omega 2019, 4, 18793−18802

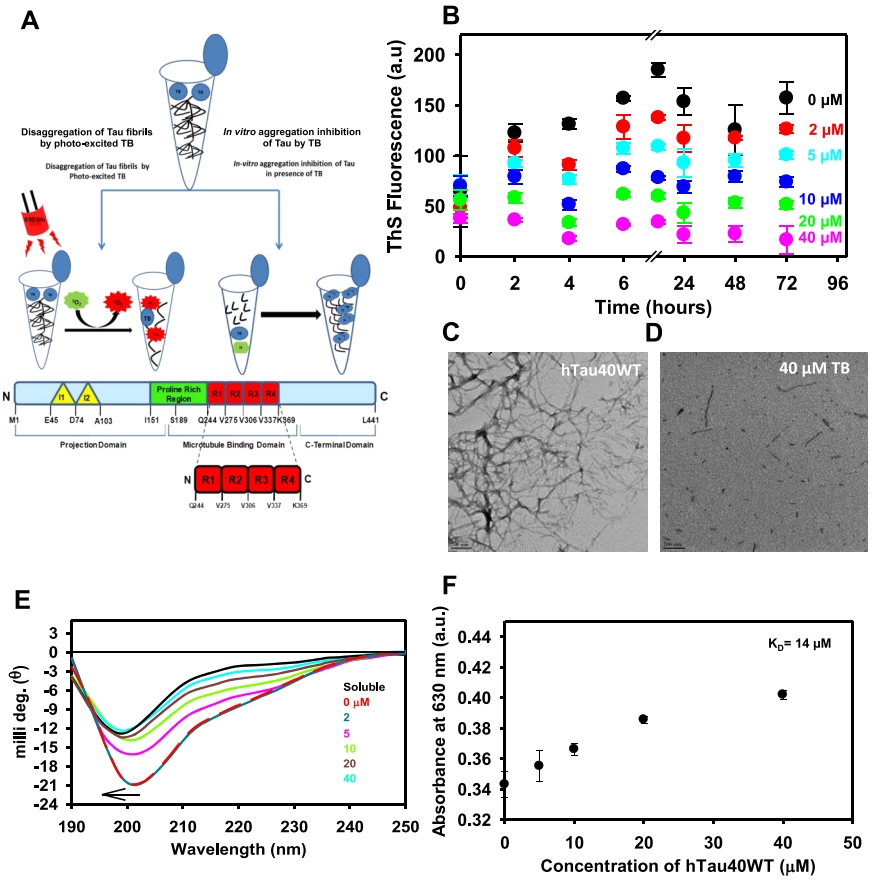

Figure 1. Tau inhibition by toluidine blue. (A) Schematic hypothesis of Tau aggregation inhibition by TB. The bar diagram demonstrates the domain organization of 441 amino acid long full-length Tau. Structurally, Tau can be divided into two domains, viz., the projection domain and the microtubule-binding domain. The four-repeat regions contribute majorly in aggregation of Tau, and the proline-rich region is a target for many post-translation modifications. (B) Effect of TB on inhibiting Tau aggregation was monitored by the ThS fluorescence assay. (C, D) Electron micrograph of Tau aggregates revealed long fibrillar morphology of Tau aggregates, whereas in the presence of TB, small broken fibrils were observed. Tau aggregates after incubating with TB exhibited the population of small, broken filaments after PDT treatment. This indicated the potency of TB in disintegrating Tau aggregates. (E) Native Tau has a random coil conformation, but as it aggregates, it attains a β-sheet conformation. Treatment with TB inhibited the conformational change in Tau, in concentration-dependent manner. (F) The absorbance maximum curve of TB in the presence of Tau at a fixed wavelength of 630 nm was measured, and the hyperbolic curve with a K_D value of 14 μM was observed.

Moreover, MB inhibits oligomer formation in amyloid-β, which is more toxic and accelerates the less toxic fibril formation. HT-22 cells were used to study the role of oxidized and reduced forms of MB in neurodegenerative disorders.[16] Additionally, photoexcited MB was also found to inhibit the aggregation of Aβ. *Drosophila* has a similar organization of brain to that of humans, where Tau plays a critical role in maintaining the integrity of the cytoskeleton of neurons. The mutation of Tau protein in *Drosophila* brain leads to formation of NFTs, which mimic the tauopathy condition of human brain.[17] The earlier works have demonstrated the potency of photoexcited xanthene dyes and porphyrin dyes against Aβ aggregation. The potency of photoexcited dyes with respect to Tau aggregation has not been reported. The aim of the present work was to study the potency of TB and PE-TB against Tau aggregation and its biocompatibility. The hypothesis was evaluated using the biochemical and biophysical assays such as the ThS fluorescence assay, sodium dodecyl sulfate-polyacrylamide gel electrophoresis (SDS-PAGE), transmission electron microscopy (TEM), and circular dichroism (CD) spectroscopy. The biocompatibility of TB and PE-TB was tested in Neuro2a cells and the transgenic *Drosophila* model. The aim of the present study was to evaluate the potency of TB and PE-TB in tauopathy. The in vitro and in vivo studies suggested the potency of TB against Alzheimer's-related pathology.

RESULTS

Toluidine Blue Inhibits Tau Aggregation in Vitro. Tau protein domain organization comprises a projection domain and a microtubule-binding domain. The schematic hypothesis depicts the domain organization of full-length Tau and its interaction with TB (Figure 1A). The four-repeat region of Tau, R1 to R4, is the aggregation-prone region. The potency of TB for inhibiting in vitro Tau aggregation was studied. For the assay, the heparin-treated Tau was incubated with various concentrations of TB ranging from 0 to 40 μM. The aggregation was measured by observing ThS fluorescence at different time intervals, and the fluorescence kinetics suggested that TB showed potent Tau aggregation inhibition. The 40 μM concentration of TB was found to show appreciable inhibition of Tau assembly (Figure 1B). Moreover, the morphological changes in TB-treated Tau were studied by electron microscopy. The electron micrographs suggested long

DOI: 10.1021/acsomega.9b02792
ACS Omega 2019, 4, 18793−18802

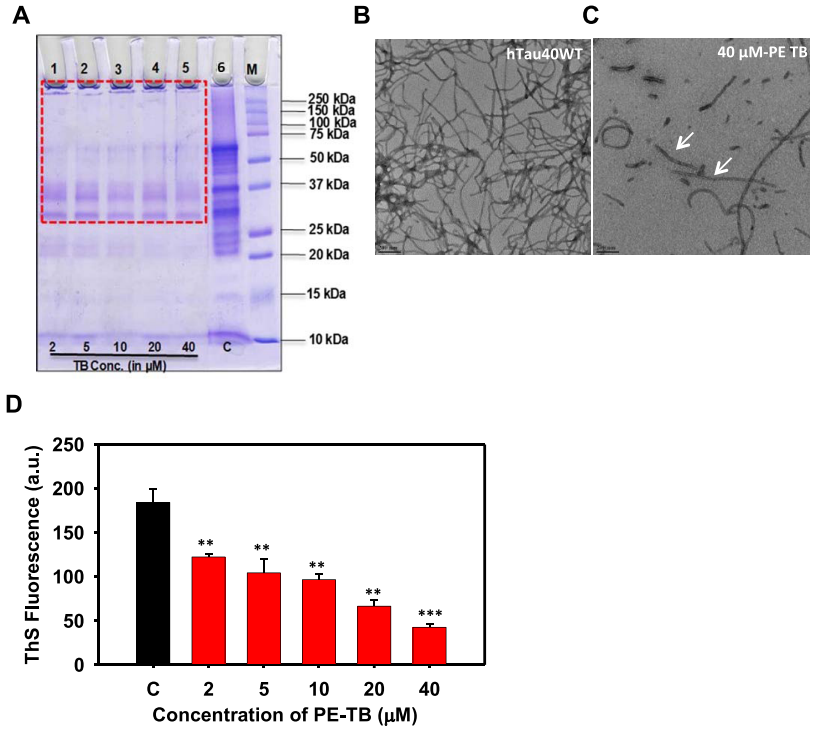

Figure 2. PE-TB disaggregates the mature Tau fibrils. (A) SDS-PAGE analysis of Tau aggregates treated with varying concentrations of PE-TB ranging from 2 to 40 μM demonstrates a clear decrease in higher-order aggregates. These results indicate the effective role of PDT against higher-order aggregates. The red box indicates the disappearance of higher-order aggregates on SDS-PAGE, which was apparent in the control group. (B, C) Electron microscopy shows long, thick, matured fibrils of Tau, whereas after incubating with PE-TB, Tau exhibits the population of small, broken filaments. This indicated the potency of TB in disintegrating Tau aggregates. (D) ThS fluorescence analysis of PE-TB-treated Tau aggregates. In PDT-treated samples, the fluorescence intensity decreased drastically. Here, 40 μM TB showed the maximum effect in disaggregating the mature aggregates.

extended filamentous Tau aggregates in the control sample, whereas incubation with TB resulted in small broken pieces of Tau, which indicated the inefficacy of Tau to aggregate (Figure 1C,D). The conformation of Tau plays an important role in pathophysiology of AD. In physiological conditions, Tau has a typical random coil conformation, but during aggregation, Tau attains a β-sheet conformation that absorbs at 220 nm. In our work, the effect of TB treatment on the secondary structure of Tau was studied. The untreated Tau aggregates showed CD spectrum of a β-sheet structure, whereas the TB-treated protein was found to be random coil (Figure 1E). TB has an absorption maximum at 630 nm (Figure S1A,B). Furthermore, the binding constant of TB for Tau was measured by UV spectroscopy. The binding constant (K_D) for TB and Tau was calculated by measuring the long-range spectrum of TB on incubating with various concentrations of full-length Tau. As Tau and TB both have basic charge, TB showed low affinity for Tau. A high K_D value of 14 μM suggested a weak interaction between the dye and protein (Figure 1F).

Photoexcited Toluidine Blue Disaggregates Tau Filaments. The potency of PE-TB in dissolving the preformed Tau aggregates was studied by incubating mature Tau fibrils with varying concentrations of PE-TB. In present experiments, TB was irradiated with red light (630 ± 10 nm), which led to photoexcitation of TB. The effect of PE-TB on Tau disaggregation was characterized by different biochemical and biophysical methods. SDS-PAGE showed the characteristic signature of higher-order aggregates in control samples (Figure 2A), while the treated samples showed no higher-order aggregates on SDS-PAGE. These results firmly indicated the effective role of photoexcited TB in destabilizing preformed Tau aggregates in vitro. Moreover, TEM studies indicated the disaggregation potency of PE-TB for Tau, as Tau aggregates were disassembled into short and fragile aggregates (Figure 2B,C). The ThS fluorescence assay suggested that PE-TB potentially reduces the Tau fibrils as a decrease in fluorescence intensity was observed in a concentration-dependent manner (Figure 2 D). Here, we speculate that the disaggregation potency of PE-TB could be a cumulative effect of TB and the singlet oxygen species produced after photoexcitation.

Biocompatibility and Toxicity of TB. TB is a photosensitizer; thus, the efficiency of TB to produce singlet oxygen species in cells was estimated by the fluorometric 2′,7′-dichlorofluoresceindiacetate (DCFDA) assay. In our work, neuronal cells were treated with various concentrations of PE-TB and TB (Figures 3A and S2A) ranging from 0.025 to 2.5 μM. The results indicated the neuroprotective property of TB, as it generated low reactive oxygen species (ROS) levels. The effect of TB and PE-TB was studied for cellular toxicity. The methylthiazolyldiphenyl-tetrazolium bromide (MTT) assay suggested that in the presence of TB the viability of cells was rescued in the Tau-stressed group (Figures 3B and S2B). TB-treated cells were exposed to 10 min of irradiation so as to observe the cytotoxicity of PE-TB. The results suggested that PE-TB was not toxic to cells up to 500 nM, but the high concentration of PE-TB was found to be toxic. The results suggested that viability of Tau-assaulted Neuro2a cells was rescued in the presence of PE-TB. Morphologically, no distinguished change was observed after the TB treatment, but the PE-TB treatment at lower concentration (500 nM) led

DOI: 10.1021/acsomega.9b02792
ACS Omega 2019, 4, 18793−18802

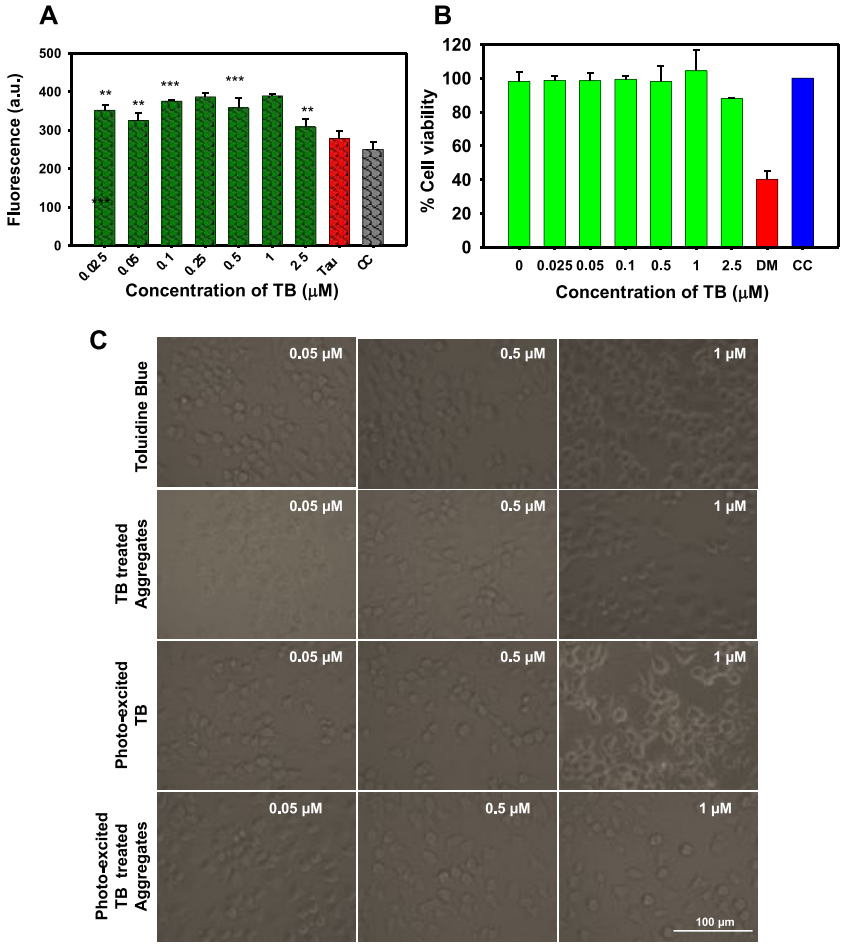

Figure 3. Biocompatibility of PE-TB. (A) The DCFDA assay indicated the extent of ROS production by PE-TB in Neuro2a cells treated with 2.5 μM Tau aggregates. These data suggest that in the presence of TB low levels of ROS were produced. (B) MTT analysis showed that the presence of TB rescued cell viability after exposing to Tau aggregates. PE-TB exhibited a protective role on cell viability in Tau-stressed cells. (C) Cell morphology did not alter after exposure to TB and PE-TB, which indicated healthy cells.

to the formation of neuronal outgrowths in Neuro2a cells, which was indicative of cytoskeleton modulation (Figure 3C).

Toluidine Blue Modulates the Cytoskeleton. Microtubules are the key component of the cytoskeleton network. The effect of TB on the cell cytoskeleton was studied by immunofluorescence assays. The effect of TB and PE-TB on cytoskeleton modulation was studied by targeting tubulin levels in cells. The cells treated with lower concentration of TB (0.5 μM) found to have healthy morphology with long neurite outgrowth and high tubulin expression as compared to untreated cells. On the contrary, a higher concentration of 5 μM of TB and PE-TB generates toxicity to the cells, leading to change in cell morphology. Additionally, the cells were also tagged with the pan-Tau K9JA antibody to observe the levels of Tau expression. The treatment showed increased Tau expression, which supports the fact that PE-TB modulates the cytoskeleton network. The fluorescence images of single neuronal cells clearly indicated that distribution of tubulin and Tau was increased after the PDT treatment. The distribution of Tau and tubulin in neurons was clearly observed in the florescent microscopic images of single neuronal cells (Figure 4).

Effect of TB and PE-TB on Transgenic *Drosophila* Model. The overexpression of Tau in the nervous system of *Drosophila* mimics tauopathy, i.e., the neuronal accumulation of Tau aggregates leading to abnormal behavior. The effect of TB and PE-TB on various behavioral aspects of UAS-E14 Tau mutant *Drosophila* was studied. *Drosophila* behavioral studies were carried out in two sets: the first set was with TB and the other was with PE-TB. The parameters chosen for the studies were feeding behavior, locomotory dysfunction, and loss of memory and potency to reproduce. The current data suggest that PE-TB has a rescuing effect on transgenic flies (Figure 5A). The flies treated with PE-TB showed increased food uptake when compared to the group exposed to TB. There was no concentration-dependent change in either set of TB exposure (Figure 5B). The next set of experiments were carried out to analyze the effect of TB and PE-TB on olfactory sensation of *Drosophila* larvae, that is, basically, the ability to avoid bad odor. The objective behind the experiment was to check the memory deficit in UAS Tau E14 transgenic *Drosophila* larvae after treatment with dye. The transgenic UAS Tau E14 larvae were unable to avoid the odor efficiently as compared to wild-type flies. The TB treatment restored olfactory sensation, indicating the potency of TB to affect the nervous system of E14 Tau *Drosophila*. Here, the photoexcited dye showed more potency over non-photoexcited TB. In the case of concentration-dependent treatment, a bell-shaped pattern was observed, which indicates that 5 μM PE-TB has maximum activity in restoring olfactory sensation of flies

DOI: 10.1021/acsomega.9b02792
ACS Omega 2019, 4, 18793−18802

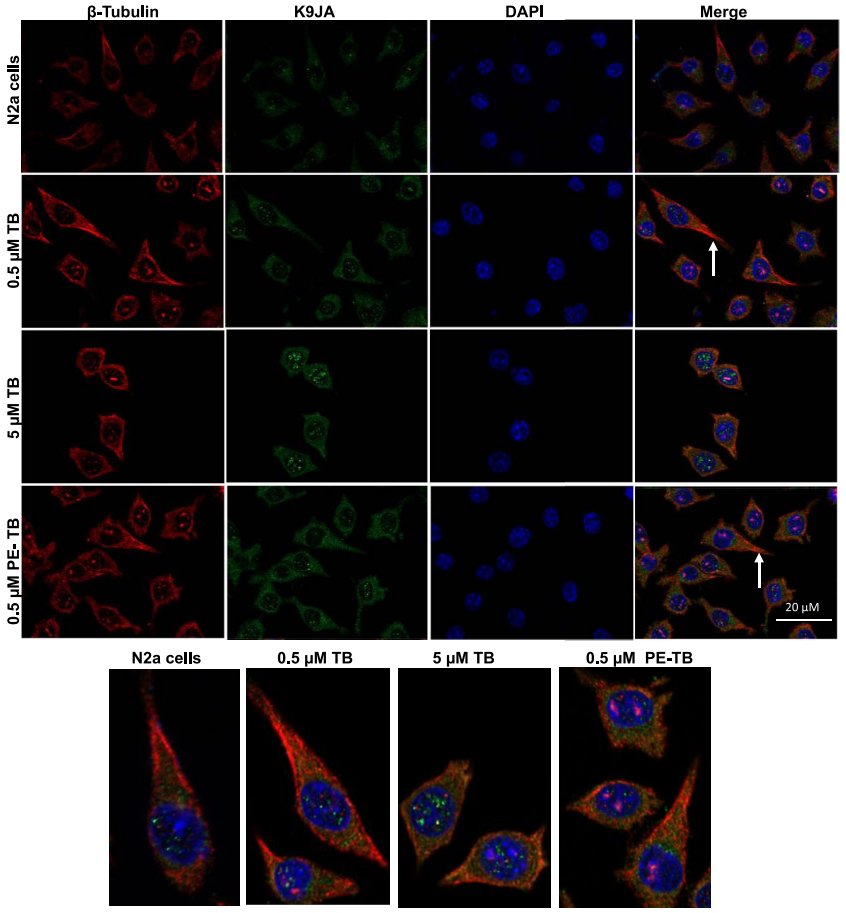

Figure 4. Modulation of the cytoskeleton network by PE-TB. The cells were treated with various concentrations of TB. At lower concentration, TB (0.5 μM) showed high expression of tubulin with increased neurite outgrowth, whereas high TB concentration (5 μM) was found to be toxic to cells. PE-TB also showed extended neurite outgrowth at lower concentration, whereas 5 μM PE-TB was cytotoxic. The fluorescent image of a tubulin-stained single neuronal cell suggested that distribution of tubulin was prominently in neurite outgrowths and Tau was distributed in the cell soma.

(Figure 5C). Succeeding experiments were performed to examine the effect of TB and PE-TB on the locomotor system in Tau flies. The negative geotaxis assay was performed, and the numbers of flies escaped were plotted against the time to interpret results in terms of percentage. The results showed a similar bell-shaped pattern as in the earlier experiment. The 5 μM concentration of PE-TB was estimated to be potent for rehabilitating the locomotor activity of flies (Figure 5D). Furthermore, the effect of TB and PE-TB was observed on the longevity of flies. For this objective, two assays, viz., the viability assay and fecundity assay, were carried out. It was observed that PE-TB increases the longevity of flies more efficiently than TB. After the treatment of dye, survival and egg laying ability of flies increased and a bell-shaped pattern was observed, indicating the efficiency of 5 μM dye to increase survival of tauopathy *Drosophila* mutant UAS Tau E14 flies (Figures 5E and S3). The overall experimental data concluded that TB was effective in restoring the adverse effect of tauopathy in Tau E14 flies. Additionally, PE-TB was more effective than non-photo-excited TB. Of all concentrations, 5 μM concentration of TB and PE-TB was found to be optimal and most effective in treating *Drosophila* tauopathy.

DISCUSSION

Pathological Tau leads to generation of paired helical filaments (PHFs), which are characteristic features of AD.[8] The importance of small molecules has been reported, which include synthetic and naturally originated compounds.[18,19] Dyes were tested thoroughly for their medicinal property because of being inexpensive, highly specific, and more potent. Their photoexcitation property was explored against various protein aggregates including Aβ, Tau, Prion, etc.[12,20,21] Toluidine blue is a phenothiazine dye, which was known to decrease the AD pathology. TB was reported to decrease the secretion of pathological Aβ-40 and Aβ-42.[22] Furthermore, TB was found to modulate the amyloid-protein-mediated pathology in hippocampus; on the contrary, TB was unable to rescue the Tau phosphorylation in transgenic 3 × Tg mice.[22] Moreover, in the present study, we investigated the effects of TB and PE-TB against Tau aggregation. MB, the parent compound of TB, has been reported in the literature as a potent Tau aggregation inhibitor. In our experiments, the K_D value of 14 μM indicated weak binding affinity of TB for Tau, which could be due to the basic charge of TB. However, in this contemporary study, the potency of PE-TB in dissolving the preformed Tau aggregates has also been analyzed by various biochemical and biophysical methods such as ThS fluorescence, SDS-PAGE, CD spectroscopy, and electron micros-

DOI: 10.1021/acsomega.9b02792
ACS Omega 2019, 4, 18793−18802

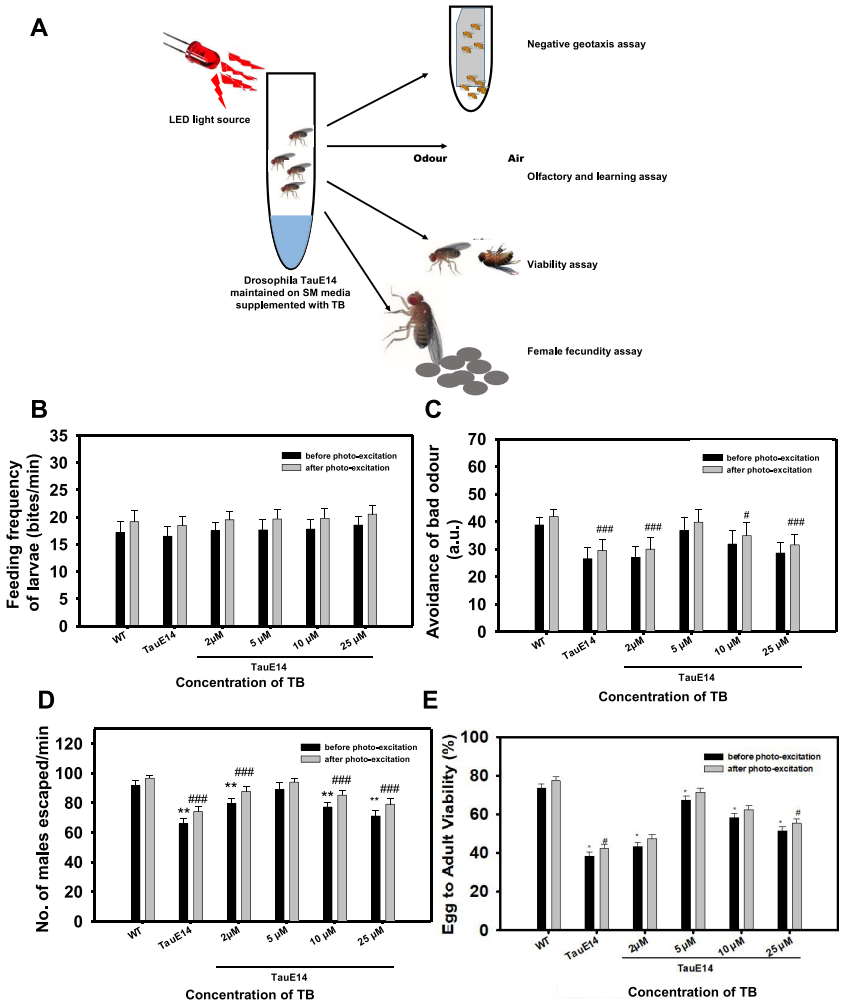

Figure 5. Effect of TB and PE-TB on behavior of transgenic *Drosophila*. (A) Transgenic flies were exposed to TB and PE-TB for various time points at different stages of life cycle to study their effect in restoring memory deficit, locomotory dysfunction, and viability. (B) Results suggest the effect of various concentrations of TB and PE-TB on feeding behavior of flies. PE-TB was found to be more potent than non-photo-excited TB. (C) E14 Tau flies were exposed to various concentrations of TB to analyze changes in olfactory sensation by avoiding the bad odor of quinine. The 5 μM concentration of PE-TB demonstrated appreciable potency in restoring the olfaction. (D) Negative geotaxis assay was performed to examine the effect of TB on locomotion of flies. The bell-shaped graph indicated 5 μM PE-TB to be effective in rescuing the locomotory system of E14 Tau *Drosophila*. (E) Data indicates 5 μM TB to have appreciable effect on the survival rate of transgenic flies. The significance was calculated using Student's *t*-test in SigmaPlot 10.0, where $^{*}p < 0.05$, $^{**}p < 0.001$, and $^{***}p < 0.0001$, the statistical difference between control and treated groups before photoexcitation, and $^{\#}p < 0.05$, $^{\#\#}p < 0.001$, and $^{\#\#\#}p < 0.0001$, the statistical difference between control and treated groups after photoexcitation.

copy. Additionally, TB possesses the tendency of photo-excitation like its parent compound MB and exposure at 630 nm leads to generation of singlet oxygen species.[23] The ThS binding revealed the role of TB in inhibiting the aggregation of Tau. The aggregates formed were analyzed qualitatively using TEM, which details the effect of small molecules on the aggregate morphology. The phenothiazine dye MB effectively inhibited Tau aggregate formation.[24] However, other dyes such as methyl yellow, azo dye, and ponceau, a sulfonated dye, had no effect on Tau aggregation.[25] The morphology of Tau in the presence of TB evidenced the potential in preventing aggregate formation, resulting in fragmented filaments. The protein loses its native conformation during aggregation, and this was shown by change in absorbance in the far-UV region. Studies showed that photoexcited MB prevented the conformational changes in Aβ from a random coil to a β-sheet-rich structure.[26] Similarly, TB also prevented conformational changes in Tau and maintained its random coil conformation. Generation of singlet oxygen species is a characteristic of a photosensitizer, and being a potent photosensitizer, TB generates singlet oxygen.[27,28] TB is a reported photosensitizer; thus, the levels of ROS produced by PE-TB have been studied. The minimal generation of ROS by PE-TB projects it as a biocompatible photosensitizer, which can be further implied in vivo to check its efficiency. Protein aggregates are known to induce oxidative stress in cells.[29−31] Thus, we studied the effect of TB in the context of ROS production, and the result suggested that in Tau-stressed cells low levels of ROS generated in the presence of TB. A dye is considered as biocompatible if it generates low levels of toxicity in cells.[32] Our findings suggested that TB has moderate cytotoxic potency at lower concentrations. Additionally, it protects cells from oxidative stress and other toxic insults.[33] Similar results were observed in the present experiments, which evidenced TB to be nontoxic in Neuro2a cells up to a sub-micro-molar level. There are studies suggesting the fact that treatment with natural compounds

DOI: 10.1021/acsomega.9b02792
ACS Omega 2019, 4, 18793−18802

such as curcumin and resveratrol increases the neurite outgrowths and helps in proliferation of cells.[34] Similarly, the high throughput screening of cerivastatin identified it as a neurite growth accelerator.[35] Likewise in our experiments, TB and PE-TB were found to increase the neurite outgrowth in Neuro2a cells. *Drosophila* has been proven to be an ideal model for neurodegenerative diseases. Several mutants of drosophila have been reported in the context to tauopathy.[36] Recently, the studies stated that photoexcited MB decreased the vacuole formation in *Drosophila* brain, indicating the rescue from neurodegeneration.[37] Human Tau pathology has been effectively modeled in *Drosophila*, which was based on overexpression of mutant Tau in fly brain. PE-TB rescued the tauopathy in *Drosophila*. We found that PE-TB reversed tauopathy-induced neurodegenerative phenotypic disorders like olfactory disability, reproductive potentiality, loss of memory, and locomotory disability in UAS Tau E14 *Drosophila* mutants. The behavioral deficits were targeted for studying the effect of Tau expression in *Drosophila* neurons. These results indicate that PE-TB could suppress behavioral defects by reducing the formation of Tau aggregates in *Drosophila* brain. Collectively, behavioral analysis in *Drosophila* indicates that tauopathy-induced behavioral defects were rescued after TB treatment. Neurons are essential for olfactory learning, which is elicited by memory retrieval or stability. This underlies the cognitive deficits observed early in many tauopathies. The overall studies on TB in various in vitro and in vivo systems strongly support its efficiency against AD-related tauopathy.

CONCLUSIONS

The Tau aggregates are considered to be one of the leading causes of AD. Thus, for studying a new therapeutic molecule for AD, Tau aggregates are being targeted. We investigated the potency of TB against Tau aggregation, and the results of all of the studies suggested that TB possesses a dual property of aggregation inhibition and disaggregation. In this study, we addressed, for the first time, the role of PE-TB against mature Tau aggregates. The in vitro assays supported that PE-TB has potency to dissolve the pathological Tau fibrils. Additionally, the low levels of singlet oxygen species generation by PE-TB make the dye more appropriate for administration in a biological system. The in vivo studies on the *Drosophila* model of tauopathy also supported TB as well as PE-TB to be a biocompatible molecule. The overall results of our study provide evidence to support the efficiency of TB as well as PE-TB as a novel molecule against tauopathy.

MATERIALS AND METHODS

Chemicals and Reagents. MES, heparin, BES, bicinchoninic acid (BCA), $CuSO_4$, thioflavin S (ThS), ANS, toluidine blue, MTT, and dimethyl sulfoxide (DMSO) were purchased from Sigma. IPTG and dithiothreitol (DTT) were purchased from Calbiochem. Other chemicals such as ampicillin, NaCl, KCl, Na_2HPO_4, KH_2PO_4, ethylene glycol tetraacetic acid (EGTA), $MgCl_2$, phenylmethylsulfonyl fluoride (PMSF), ammonium acetate, and bovine serum albumin (BSA) were obtained from MP and protease inhibitor cocktail was obtained from Roche. Copper-coated carbon grids were purchased from Ted Pella, Inc. Advanced DMEM/F-12 media, fetal bovine serum (FBS), pensterp cocktail, and anti-anti were purchased from Gibco. All laboratory reagents used for *Drosophila* studies were purchased from Merck.

Recombinant Preparation of Tau. The recombinant full-length Tau was purified as per the published protocol.[11] Briefly, the recombinant full-length Tau was expressed in the *Escherichia coli* BL21* strain. The cells were grown at 37 °C till the OD_{600} reached 0.5 to 0.6. They were then induced with 0.5 mM IPTG and were further incubated for 4 h and harvested by centrifugation at 4000 rpm for 10 min. The protein isolation and purification were done as described previously.[38] The lysing of cells was done using homogenizer constant cell disruption systems. The cells were resuspended in buffer A composed of 50 mM MES, 1 mM EGTA, 2 mM $MgCl_2$, 5 mM DTT, 1 mM PMSF, and 50 mM NaCl and were subjected to homogenization at 15 000 psi pressure. The obtained lysate was heated at 90 °C for 20 min in the presence of 0.5 M NaCl and 5 mM DTT. This was cooled and centrifuged at 40 000 rpm for 45 min. The supernatant was collected and dialyzed overnight against buffer A before loading to a cation exchange column. Increasing the ionic gradient of NaCl to 1 M, the Tau protein was eluted. The protein quality was analyzed by SDS-PAGE, and the protein was further passed through size exclusion chromatography columns. The obtained protein was analyzed, pooled, and concentrated. The concentration was estimated by the BCA assay, and the protein was stored at −80 °C till further use. Tau aggregation was induced at 37 °C with heparin as previously described.[39] Tau in the presence of an anionic inducer such as heparin, RNA, arachidonic acid, etc. undergoes aggregation. Among all of these molecules, the heparin-induced Tau aggregation is a widely accepted model for in vitro tauopathy studies. Earlier studies suggested the heparin-mediated Tau aggregation model to demonstrate the transition of Tau from random coil to β-sheets upon aggregation.[40] Taniguchi et al. demonstrate the inhibition of heparin-induced Tau filaments by phenothiazine, polyphenols, and porphyrins.[25] In the present work, Tau aggregation was induced by heparin where the soluble full-length Tau was mixed with heparin (17 500 Da) at a ratio of 4:1. The reaction was carried out in 20 mM BES buffer supplemented with 25 mM NaCl, 1 mM DTT, and 0.01% NaN_3 and protease inhibitor cocktail mixtures.

Thioflavin S Fluorescence Assay. The effect of TB on the aggregation property of Tau was measured by the thioflavin S (ThS) fluorescence assay.[10] ThS is a mixture of methylated dehydrothiotoluidine and sulfonic acid and has the property to fluoresce on binding to β-sheet structures. The fluorescence measurement was carried out by incubating 2 μM Tau with ThS in a 1:4 ratio for 15 min in the dark. All of the reaction mixtures were measured in triplicate, in a TECAN Infinite M200 PRO spectrophotometer, at an excitation of 440 nm and emission of 521 nm. Further, the data was analyzed using SigmaPlot 10.0.

Circular Dichroism Spectroscopy. The conformational changes in Tau were analyzed using CD spectroscopy in the far-UV region. In native conditions, Tau has a typical random coil conformation, but the aggregation causes a conformational change to β-sheet, which absorbs at around 220 nm. The effect of TB on conformational changes in Tau was studied as described previously.[41] All of the spectra were measured in a Jasco J-815 spectrometer by diluting full-length Tau to 3 μM in 50 mM phosphate buffer at pH 6.8.

Binding Constant. The binding constant of TB with Tau was estimated by UV−visible spectroscopy. The experiment

DOI: 10.1021/acsomega.9b02792
ACS Omega 2019, 4, 18793−18802

was performed using a 96-well clear bottom plate (Eppendorf), and measurements were recorded in a Tecan Infinite M200 PRO spectrophotometer. TB (20 μM) was incubated with varying concentrations of Tau (0, 10, 20, 30, 40, and 50 μM). The binding constant (K_D) value was calculated after recording the spectrum ranging from 230 to 800 nm. The absorption maximum of Tau was observed at 314 nm. All of the samples were diluted in phosphate buffer, at pH 6.8.

$$[PL] = \frac{[P_o] \times [L]}{K_D + [L]}$$

Here, $[P_0]$ is the initial protein concentration, $[L]$ is the free ligand concentration, $[PL]$ is the concentration of the protein−ligand complex, and K_D is the dissociation constant.

Light-Induced Inhibition of Tau Assembly. For analyzing the effect of photoexcited TB on Tau aggregates, aggregates were incubated for 1 h in the dark with varying concentrations of TB (2, 5, 10, 20, and 40 μM). Then, 200 μL of the reaction mixture was added in a 96-well black plate (Eppendorf) and was irradiated in the dark using red LED. After 1 h of incubation, the samples were analyzed by ThS fluorescence and SDS-PAGE for the presence of disintegrated Tau.

Light-Induced Inhibition of Tau Aggregates Analyzed by SDS-PAGE. The inhibitory effect of TB on Tau aggregation was observed by SDS-PAGE. Various TB-treated reaction mixtures were analyzed. Aggregates have a characteristic pattern of higher molecular weights around 250 kDa; thus, the effect of TB on aggregation propensity of Tau can be easily observed by SDS-PAGE. The experiments were performed using a GE miniVE electrophoresis unit and a BIORAD Mini-PROTEAN electrophoresis unit.

Transmission Electron Microscopy. The morphological analysis of Tau fibrils was done by electron microscopy, and the samples were prepared according to the published protocol.[11] For electron microscopic analysis, 2 μM Tau was incubated on carbon-coated copper grids. Following this, the samples were negatively stained with 2% uranyl acetate. The images were captured by TECNAI T20 at 120 kV.

ROS Production in Neuro2a Cells. The effect of photoexcited TB on ROS production was estimated in Neuro2a cells using the 2′,7′-dichlorofluoresceindiacetate (DCFDA) assay.[42,43] ROS oxidizes 2,7-dichlorofluorescindiacetate to 2′,7′-dichlorofluorescein (DCF), leading to the generation of fluorescence. For the assay, 10 000 cells/well were seeded in a 96-well plate and incubated for 24 h. The cells were treated with various concentrations of TB following 10 min of irradiation in the dark. After treatment, the cells were washed twice with 1× PBS (pH 7.4), supplemented with 10 μM DCFDA, and incubated for 20 min. After incubation, the cells were again washed twice with 1× PBS. Finally, 100 μL of phenol red-free Dulbecco's modified Eagle medium (DMEM) was added in each well and fluorescence was measured at 535 nm upon exciting at 485 nm.

Cytotoxicity Assay. The cell viability was analyzed by the methylthiazolyldiphenyl-tetrazolium bromide (MTT) assay.[10,44,45] Neuro2a cells were cultured in advanced DMEM/F-12 media supplemented with 10% FBS and glutamine. The cells were trypsinized with a 0.25% trypsin-EDTA solution. A total of 10 000 cells/well were seeded in 96-well plates for the assays. After 24 h, the cells were treated with various concentrations of TB for 24 h, followed by addition of MTT at a concentration of 0.5 mg/mL and incubation at 37 °C for 4 h. The formazan crystals formed were dissolved in 100 μL of 100% DMSO. Cell viability was evaluated by measuring the absorbance at 570 nm. Similarly, cells were incubated with 2.5 μM aggregates to observe the cytotoxicity of Tau aggregates; additionally, TB was also added to cells along with aggregates for analyzing the effect of TB in the presence of aggregates. TB-treated cells were subjected to 10 min of irradiation for the cytotoxicity analysis of PE-TB.

Immunofluorescence Analysis of Tubulin Expression in Neuro2a Cells. Neuro2a cells were seeded at a density of 50 000 cells on glass cover slips. The cells were treated with various concentrations of TB (0.5, 5, and 50 μM) and incubated overnight at 37 °C. Similarly, another set of cells treated with various concentrations of TB were irradiated with red light for 10 min and incubated at 37 °C. The cells were fixed with absolute methanol for 20 min at −20 °C. After fixation, cells were permeabilized by 0.2% Triton X-100. After 3 subsequent washes of PBS, the cells were incubated with 5% horse serum for 1 h. The cells were incubated with the anti-tubulin (Thermo PA1-41331) and K9JA (Dako A0024) antibody. After overnight incubation, the cells were incubated with Alexa Fluor 488 (A11034)- and Alexa Fluor 555 (A32727)-tagged secondary antibodies. The nucleus was stained with DAPI. The cells were scanned by a Zeiss Axio observer 7.0, apotome 2.0 inverted microscope using 63× magnifications in oil immersion and at 40% light intensity.

Fly Stocks and Genetics. The transgenic *Drosophila* strain used in this study was UAS Tau E14. The ELAV-Gal4 driver line was obtained from the National Drosophila Stock Center at the University of Mysore, Mysore, Karnataka, India. *Drosophila* strains were raised on standard medium. Fly cultures and crosses were carried out at 25 °C.

Fly Husbandry. Flies were maintained on standard banana-jaggery medium (SM) under standard laboratory conditions of 24 ± 1 °C temperature, 75 ± 5% relative humidity, and 12:12 light and dark cycle (SLC).[46] Flies were maintained in a 2 week discrete generation cycle for 10 generations before being used in this study. The adult density was regulated at about 100 flies per half-pint bottle with 25 mL of SM in 10 bottles. Flies from 10 bottles were combined into a single breeding cage, hereafter referred to as parental cage.

Preparation of TB-Supplemented Diet. A total of 2.5 L of SM was prepared and split into five batches of 500 mL each as described previously.[46] For the control group, SM was poured into the bottles. For the TB-supplemented media, 2.5, 5.0, 10, and 25 μM TB was added and mixed thoroughly just before pouring into the bottles. All bottles were plugged with nonadsorbent cotton, and the media were allowed to set under room temperature.

Larval Feeding Behavior Assay. The eggs obtained were transferred at a density of 50 eggs/6 mL of SM and allowed to develop till early third instar. The early third instar larvae were removed from the SM vials and used in the feeding behavior assay. Larvae were individually transferred to an assay Petri plate of 5 cm diameter containing 10 mL of either liquid SM (SM without agar) or liquid SM supplemented with different concentrations of TB and allowed to acclimate for 5 s. The feeding rate was measured as the mean number of sclerite retractions in two consecutive 30 s intervals. The average of the two rates was taken as the feeding rate of that larva. Then, 20 larvae were assayed for each of the two treatment groups. The

DOI: 10.1021/acsomega.9b02792
ACS Omega 2019, 4, 18793−18802

feeding rate assays were replicated four times. A total of 160 larvae were assayed for the feeding rate.

Fecundity Assay. Flies from the holding vials were sexed under low CO_2 anesthesia, and a single pair (one male + one female) was transferred to a vial with ∼3 mL of SM. Then, 20 such vials were set up per treatment, per population. Flies were transferred without anesthesia to fresh SM vials every 24 h, and the eggs laid during the previous 24 h were counted under a microscope and recorded. The daily egg counts were carried out till the death of female fly in each test vial.

Negative Geotaxis Assay. The ability to move against gravity and climb indicated the level of physical fitness of test animals. Vertical climbing ability of male flies that emerged from different treatment bottles was assessed. Twenty male flies per treatment group were collected and transferred to the empty, 0−15 cm graduated vial. The vial was gently tapped and placed in a vertical position. The number of flies that crossed the 15 cm mark in 30 s was counted. Three trials were conducted on each set of 20 flies. The data was expressed as percentage of flies that crossed the 15 cm mark.

Viability of Fly from Egg to Adult. The eggs from medium plates were collected and dispensed into different treatment groups of bottles at a density of ∼100 eggs/bottle with 45 mL of media. Ten bottles each for five treatment groups of SM and SM with 2, 5, 10, and 25 μM TB were prepared. Bottles were maintained at standard laboratory conditions. The flies emerged from different treatments, SM and SM with 2, 5, 10, and 25 μM TB, were designated, collected, and counted. All of the assays were carried out on SM using mated flies. The total number of flies that emerged from each bottle were used to calculate the viability of flies emerging from each treatment group.

Larval Olfactory Behavior. The olfactory test was carried out by employing the previous method with minor modifications.[47] A total of 30 larvae were briefly dried on a filter paper before being placed in the center of the Petri dish. The Petri dish containing 20 μL of quinine sulfbad odate dispensed on each of the two 0.5 cm radius filter disks were placed in a diametrically opposite position to quinine zones. After 2 min of placing the larvae and covering the Petri dish, numbers of larvae in different zones were counted to calculate the percentage of larvae avoiding the bad odor after training.

Statistical Analysis. Using either duplicate or triplicate reading, the statistical data were plotted. Untransformed (raw) data were analyzed and plotted by SigmaPlot 10.0 software. The data were analyzed for significance by Student's *t*-test, where $*p < 0.05$, $**p < 0.001$, and $***p < 0.0001$.

■ ASSOCIATED CONTENT

Supporting Information

The Supporting Information is available free of charge on the ACS Publications website at DOI: 10.1021/acsomega.9b02792.

UV absorption spectrum of TB, TB absorption in the presence of Tau, ROS production after TB exposure, effect of TB on drosophila (PDF)

■ AUTHOR INFORMATION

Corresponding Author

*E-mail: s.chinnathambi@ncl.res.in. Tel: +91-20-25902232. Fax: +91-20-25902648.

ORCID

Subashchandrabose Chinnathambi: 0000-0002-5468-2129

Author Contributions

T.D, N.V.G., and S.C. designed the experiments. T.D. and N.V.G. carried out the experiments. T.D., N.V.G., and S.C. analyzed the data and wrote the article. *Drosophila* studies were carried out by K.T.C., S.C. conceived the idea of the project. All authors contributed to the discussions and manuscript review.

Notes

The authors declare no competing financial interest.

■ ACKNOWLEDGMENTS

This project is supported in part by grants from the in-house, National Chemical Laboratory, Council of Scientific Industrial Research (CSIR-NCL) grant MLP029526. Tau constructs were kindly gifted by Prof. Roland Brandt from the University of Osnabruck, Germany. Tushar Dubey and Nalini Vijay Gorantla acknowledge the fellowship from the University Grants Commission (UGC), India.

■ ABBREVIATIONS

AD, Alzheimer's disease; PHFs, Paired Helical Filaments; NFTs, neurofibrillary tangles; TB, toluidine blue; MB, methylene blue; PDT, photodynamic therapy; ThS, thioflavin S; MTT, methylthiazolyldiphenyl-tetrazolium bromide; SEC, size exclusion chromatography; BCA, bicinchoninic acid; DMSO, dimethyl sulfoxide; DNPH, dinitrophenylhydrazine; ROS, reactive oxygen species; SDS-PAGE, sodium dodecyl sulfate-polyacrylamide gel electrophoresis; TEM, transmission electron microscopy; BSA, bovine serum albumin

■ REFERENCES

(1) Arriagada, P. V.; Growdon, J. H.; Hedley-Whyte, E. T.; Hyman, B. T. Neurofibrillary tangles but not senile plaques parallel duration and severity of Alzheimer's disease. *Neurology* **1992**, *42*, 631.

(2) Selkoe, D. J. The molecular pathology of Alzheimer's disease. *Neuron* **1991**, *6*, 487−498.

(3) Forman, M. S.; Trojanowski, J. Q.; Lee, V. M. Y. Neurodegenerative diseases: a decade of discoveries paves the way for therapeutic breakthroughs. *Nat. Med.* **2004**, *10*, 1055−1063.

(4) Morris, M.; Maeda, S.; Vossel, K.; Mucke, L. The many faces of tau. *Neuron* **2011**, *70*, 410−426.

(5) Giacobini, E.; Gold, G. Alzheimer disease therapy moving from amyloid-Î² to tau. *Nat. Rev. Neurol.* **2013**, *9*, 677−686.

(6) Mandelkow, E.-M.; Mandelkow, E. Biochemistry and cell biology of tau protein in neurofibrillary degeneration. *Cold Spring Harbor Perspect. Med.* **2012**, *2*, No. a006247.

(7) Obulesu, M.; Venu, R.; Somashekhar, R. Tau mediated neurodegeneration: an insight into Alzheimer's disease pathology. *Neurochem. Res. 36* 1329 1335. DOI: 10.1007/s11064-011-0475-5.

(8) Wang, Y.; Mandelkow, E. Tau in physiology and pathology. *Nat. Rev. Neurosci.* **2016**, *17*, 22−35.

(9) Sonawane, S. K.; Chinnathambi, S. Prion-Like Propagation of Post-Translationally Modified Tau in Alzheimer's Disease: A Hypothesis. *J. Mol. Neurosci.* **2018**, *65*, 480−490.

(10) Sonawane, S. K.; Ahmad, A.; Chinnathambi, S. Protein-Capped Metal Nanoparticles Inhibit Tau Aggregation in Alzheimer's Disease. *ACS Omega* **2019**, *4*, 12833−12840.

(11) Gorantla, N. V.; Das, R.; Mulani, F. A.; Thulasiram, H. V.; Chinnathambi, S. Neem Derivatives Inhibits Tau Aggregation. *J. Alzheimer's Dis. Rep.* **2019**, *3*, 169−178.

(12) Janouskova, O.; Rakusan, J.; Karaskova, M.; Holada, K. Photodynamic inactivation of prions by disulfonated hydroxyaluminium phthalocyanine. *J. Gen. Virol.* **2012**, *93*, 2512−2517.

(13) Lee, B. I.; Lee, S.; Suh, Y. S.; Lee, J. S.; Kim, A.; Kwon, O. Y.; Yu, K.; Park, C. B. Photoexcited Porphyrins as a Strong Suppressor of Amyloid Aggregation and Synaptic Toxicity. *Angew. Chem.* **2015**, *127*, 11634−11638.
(14) Wischik, C. M.; Harrington, C. R.; Storey, J. M. D. Tau-aggregation inhibitor therapy for Alzheimer's disease. *Biochem. Pharmacol.* **2014**, *88*, 529−539.
(15) Oz, M.; Lorke, D. E.; Petroianu, G. A. Methylene blue and Alzheimer's disease. *Biochem. Pharmacol.* **2009**, *78*, 927−932.
(16) Atamna, H.; Kumar, R. Protective role of methylene blue in Alzheimer's disease via mitochondria and cytochrome c oxidase. *J. Alzheimer's Dis.* **2010**, *20*, S439−S452.
(17) Bolkan, B. J.; Kretzschmar, D. Loss of Tau results in defects in photoreceptor development and progressive neuronal degeneration in Drosophila. *Develop. Neurobiol.* **2014**, *74*, 1210−1225.
(18) Calcul, L.; Zhang, B.; Jinwal, U. K.; Dickey, C. A.; Baker, B. J. Natural products as a rich source of tau-targeting drugs for Alzheimer's disease. *Future Med. Chem.* **2012**, *4*, 1751−1761.
(19) Pickhardt, M.; Neumann, T.; Schwizer, D.; Callaway, K.; Vendruscolo, M.; Schenk, D.; George-Hyslop, S. P.; Mandelkow, E.; Dobson, C.; McConlogue, L. Identification of small molecule inhibitors of tau aggregation by targeting monomeric tau as a potential therapeutic approach for tauopathies. *Curr. Alzheimer Res.* **2015**, *12*, 814−828.
(20) Lee, B. I.; Suh, Y. S.; Chung, Y. J.; Yu, K.; Park, C. B. Shedding Light on Alzheimer's Amyloidosis: Photosensitized Methylene Blue Inhibits Self-Assembly of Î²-Amyloid Peptides and Disintegrates Their Aggregates. *Sci. Rep.* **2017**, *7*, No. 7523.
(21) Gorantla, N. V.; Chinnathambi, S. Tau Protein Squired by Molecular Chaperones During Alzheimer's Disease. *J. Mol. Neurosci.* **2018**, *66*, 356−368.
(22) Yuksel, M.; Biberoglu, K.; Onder, S.; Akbulut, K. G.; Tacal, O. Effects of phenothiazine-structured compounds on APP processing in Alzheimer's disease cellular model. *Biochimie* **2017**, *138*, 82−89.
(23) Page, K.; Wilson, M.; Parkin, I. P. Antimicrobial surfaces and their potential in reducing the role of the inanimate environment in the incidence of hospital-acquired infections. *J. Mater. Chem.* **2009**, *19*, 3819−3831.
(24) Wischik, C. M.; Edwards, P. C.; Lai, R. Y.; Roth, M.; Harrington, C. R. Selective inhibition of Alzheimer disease-like tau aggregation by phenothiazines. *Proc. Natl. Acad. Sci. U.S.A.* **1996**, *93*, 11213−11218.
(25) Taniguchi, S.; Suzuki, N.; Masuda, M.; Hisanaga, S.-i.; Iwatsubo, T.; Goedert, M.; Hasegawa, M. , Inhibition of heparin-induced tau filament formation by phenothiazines, polyphenols, and porphyrins. *J. Biol. Chem.* **2005**, *280*, 7614−7623.
(26) Akoury, E.; Pickhardt, M.; Gajda, M.; Biernat, J.; Mandelkow, E.; Zweckstetter, M. Mechanistic basis of phenothiazinedriven inhibition of Tau aggregation. *Angew. Chem., Int. Ed.* **2013**, *52*, 3511−3515.
(27) Komerik, N.; Nakanishi, H.; MacRobert, A. J.; Henderson, B.; Speight, P.; Wilson, M. In vivo killing of Porphyromonas gingivalis by toluidine blue-mediated photosensitization in an animal model. *Antimicrob. Agents Chemother.* **2003**, *47*, 932−940.
(28) Bouillaguet, S.; Wataha, J. C.; Zapata, O.; Campo, M.; Lange, N.; Schrenzel, J. Production of reactive oxygen species from photosensitizers activated with visible light sources available in dental offices. *Photomed. Laser Surg.* **2010**, *28*, 519−525.
(29) Zhang, W.; Wang, T.; Pei, Z.; Miller, D. S.; Wu, X.; Block, M. L.; Wilson, B.; Zhang, W.; Zhou, Y.; Hong, J.-S.; et al. Aggregated α-synuclein activates microglia: a process leading to disease progression in Parkinson's disease. *FASEB J.* **2005**, *19*, 533−542.
(30) Schilling, T.; Eder, C. Amyloid β induced reactive oxygen species production and priming are differentially regulated by ion channels in microglia. *J. Cell. Physiol.* **2011**, *226*, 3295−3302.
(31) Zraika, S.; Hull, R. L.; Udayasankar, J.; Aston-Mourney, K.; Subramanian, S. L.; Kisilevsky, R.; Szarek, W. A.; Kahn, S. E. Oxidative stress is induced by islet amyloid formation and time-dependently mediates amyloid-induced beta cell apoptosis. *Diabetologia* **2009**, *52*, 626−635.
(32) Tremblay, J.-F. O.; Dussault, S.; Viau, G.; Gad, F.; Boushira, M.; Bissonnette, R. Photodynamic therapy with toluidine blue in Jurkat cells: cytotoxicity, subcellular localization and apoptosis induction. *Photochem. Photobiol. Sci.* **2002**, *1*, 852−856.
(33) Harrington, C. R.; Storey, J. M. D.; Clunas, S.; Harrington, K. A.; Horsley, D.; Ishaq, A.; Kemp, S. J.; Larch, C. P.; Marshall, C.; Nicoll, S. L. Cellular models of aggregation-dependent template-directed proteolysis to characterize tau aggregation inhibitors for treatment of Alzheimer disease. *J. Biol. Chem.* **2015**, *290*, 10862−10875.
(34) Bora-Tatar, G.; Erdem-Yurter, H. Investigations of curcumin and resveratrol on neurite outgrowth: perspectives on spinal muscular atrophy. *BioMed Res. Int.* **2014**, No. 709108.
(35) Sherman, S. P.; Bang, A. G. High-throughput screen for compounds that modulate neurite growth of human induced pluripotent stem cell derived neurons. *Dis. Models Mech.* **2018**, No. 031906.
(36) Iijima-Ando, K.; Iijima, K. Transgenic Drosophila models of Alzheimer's disease and tauopathies. *Brain Struct. Funct.* **2010**, *214*, 245−262.
(37) Lee, B. I.; Suh, Y. S.; Chung, Y. J.; Yu, K.; Park, C. B. Shedding Light on Alzheimer's β-Amyloidosis: Photosensitized Methylene Blue Inhibits Self-Assembly of β-Amyloid Peptides and Disintegrates Their Aggregates. *Sci. Rep.* **2017**, *7*, No. 7523.
(38) Gorantla, N. V.; Khandelwal, P.; Poddar, P.; Chinnathambi, S. Global Conformation of Tau Protein Mapped by Raman Spectroscopy. In *Tau Protein: Methods and Protocols*; Humana Press: NY, pp 21−31.
(39) Barghorn, S.; Biernat, J.; Mandelkow, E. Purification of Recombinant Tau Protein and Preparation of Alzheimer-Paired Helical Filaments in Vitro. In *Amyloid Proteins: Methods and Protocols*; Humana Press: NY, 2005; pp 35−51.
(40) Barghorn, S.; Biernat, J.; Mandelkow, E. Purification of Recombinant Tau Protein and Preparation of Alzheimer-Paired Helical Filaments in Vitro. In *Amyloid Proteins*; Springer, 2005; pp 35−51.
(41) Gorantla, N. V.; Shkumatov, A. V.; Chinnathambi, S. Conformational Dynamics of Intracellular Tau Protein Revealed by CD and SAXS. In *Tau Protein: Methods and Protocols*; Humana Press: NY, pp 3−20.
(42) Alexandre, J.; Batteux, F.; Nicco, C.; Chreau, C.; Laurent, A.; Guillevin, L.; Weill, B.; Goldwasser, F. Accumulation of hydrogen peroxide is an early and crucial step for paclitaxel induced cancer cell death both in vitro and in vivo. *Int. J. Cancer* **2006**, *119*, 41−48.
(43) Degli Esposti, M. Measuring mitochondrial reactive oxygen species. *Methods* **2002**, *26*, 335−340.
(44) Pasinelli, P.; Borchelt, D. R.; Houseweart, M. K.; Cleveland, D. W.; Brown, R. H. Caspase-1 is activated in neural cells and tissue with amyotrophic lateral sclerosis-associated mutations in copper-zinc superoxide dismutase. *Proc. Natl. Acad. Sci. U.S.A.* **1998**, *95*, 15763−15768.
(45) Fioriti, L.; Dossena, S.; Stewart, L. R.; Stewart, R. S.; Harris, D. A.; Forloni, G.; Chiesa, R. Cytosolic prion protein (PrP) is not toxic in N2a cells and primary neurons expressing pathogenic PrP mutations. *J. Biol. Chem.* **2005**, *280*, 11320−11328.
(46) Chandrashekara, K. T.; Shakarad, M. N. Aloe vera or resveratrol supplementation in larval diet delays adult aging in the fruit fly, Drosophila melanogaster. *J. Gerontol., Ser. A* **2011**, *66*, 965−971.
(47) Heisenberg, M.; Borst, A.; Wagner, S.; Byers, D. Drosophila mushroom body mutants are deficient in olfactory learning. *J. Neurogenet.* **1985**, *2*, 1−30.

DOI: 10.1021/acsomega.9b02792
ACS Omega 2019, 4, 18793−18802